

**DOE/ID/13547**

**ELIMINATION OF THE CALCIUM CYCLE:  
DIRECT ELECTROLYTIC CAUSTICIZING OF KRAFT SMELT**

**Final Report**

**P. Pfromm  
J. Winnick**

**January 1999**

**Work Performed Under Contract No. DE-FC07-97ID13547**

**For  
U.S. Department of Energy  
Assistant Secretary for  
Energy Efficiency and Renewable Energy  
Washington, DC**

**By  
The Institute of Paper Science and Technology, Atlanta, GA  
Georgia Institute of Technology, Atlanta, GA**

**RECEIVED**  
**JAN 28 1999**  
**OSTI**  
**DOE/ID/13547**

**ELIMINATION OF THE CALCIUM CYCLE:  
DIRECT ELECTROLYTIC CAUSTICIZING OF KRAFT SMELT**

**Final Report**

**P. Pfromm  
J. Winnick**

**January 1999**

**Work Performed Under Contract No. DE-FC07-97ID13547**

**Prepared for the  
U.S. Department of Energy  
Assistant Secretary for  
Energy Efficiency and Renewable Energy  
Washington, DC**

**Prepared by  
The Institute of Paper Science and Technology, Atlanta, GA  
Georgia Institute of Technology, Atlanta, GA**

## **DISCLAIMER**

This report was prepared as an account of work sponsored by an agency of the United States Government. Neither the United States Government nor any agency thereof, nor any of their employees, make any warranty, express or implied, or assumes any legal liability or responsibility for the accuracy, completeness, or usefulness of any information, apparatus, product, or process disclosed, or represents that its use would not infringe privately owned rights. Reference herein to any specific commercial product, process, or service by trade name, trademark, manufacturer, or otherwise does not necessarily constitute or imply its endorsement, recommendation, or favoring by the United States Government or any agency thereof. The views and opinions of authors expressed herein do not necessarily state or reflect those of the United States Government or any agency thereof.

## **DISCLAIMER**

**Portions of this document may be illegible in electronic image products. Images are produced from the best available original document.**

**Final Report to the Department of Energy**

**Elimination of the Calcium Cycle: Direct Electrolytic  
Causticizing of Kraft Smelt**

DE-FC07-97-ID13547

Peter Pfromm, Institute of Paper Science and Technology, Atlanta, GA  
404-894-5305, peter.pfromm@ipst.edu

Jack Winnick, Georgia Institute of Technology, Atlanta, GA

**Abstract**

An electrochemical molten salt alternative to the classic Kraft causticizing process has been investigated and the feasibility of the process was successfully shown. The experiments include (A) the determination of background thermal decomposition gases, (B) the electrolysis of a sodium carbonate only smelt to show that sodium oxide can be electrochemically produced, and (C) electrolysis of a synthetic smelt containing 80 mole %  $\text{Na}_2\text{CO}_3$  and 20 mole %  $\text{Na}_2\text{S}$ . The experiments show that sodium hydroxide ( $\text{NaOH}$ ) was produced by the electrochemical reduction of sodium carbonate to sodium oxide in the molten state. In the experiment containing sodium sulfide, there was formation of less than 5 mole % of polysulfide.

Energy savings on the order of 500,000 BTU per ton of kraft pulp produced are estimated, based on the energy used by the mill. Operating costs are estimated to be currently similar to conventional processing. However, price increases of fossil fuels and increased co-generation of electricity in the mill will give the electrolytical process significant cost advantages.

## Table of Contents

<i>Abstract</i> .....	1
<i>Introduction</i> .....	3
<i>Background and theory</i> .....	3
<i>Experimental</i> .....	6
<b>Materials</b> .....	6
<b>Apparatus</b> .....	6
<b>Procedure</b> .....	8
<i>Results and discussion</i> .....	10
<b>Experiment A: Sodium Carbonate Melt, No Electricity</b> .....	11
<b>Experiment B: Molten Sodium Carbonate Electrolysis</b> .....	12
<b>Experiment C: Electrolysis of a Synthetic Molten Smelt</b> .....	15
<i>Comparison of the electrolytic process with the conventional process</i> .....	19
<i>Conclusions</i> .....	20
<i>Table of Figures</i> .....	22
<i>Table of Tables</i> .....	23
<i>Figures</i> .....	24
<i>Tables</i> .....	34

## **Introduction**

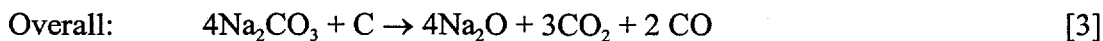
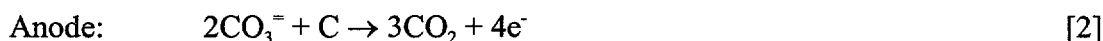
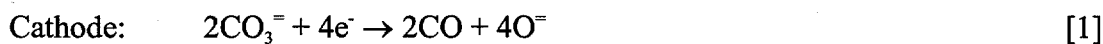
A one-step, molten sodium carbonate electrolysis alternative to the classical Kraft causticizing process has been tested for electrochemical feasibility in a batch scale cell. Chemical recovery problems alleviated by the proposed electrochemical process include the reduction of Non-Process Elements due to the absence of calcium carbonate. The reduction of the sodium carbonate deadload would also decrease since the aqueous chemical equilibrium limit to causticizing would be removed by the electrochemistry. A molten salt electrochemical cell would allow for incremental capacity increase of recovery chemicals and require a low operating voltage due to the high conductivity of molten (non-aqueous) smelt at recovery boiler temperatures (~900°C). Simplifications obtained by the molten salt electrochemical process over the classical Kraft causticizing process are presented schematically in Figures 1 & 2.

## **Background and theory**

Kraft smelts from the recovery boiler contain a mixture of sodium carbonate ( $\text{Na}_2\text{CO}_3$ ), sodium sulfide ( $\text{Na}_2\text{S}$ ), sodium sulfate ( $\text{Na}_2\text{SO}_4$ ), and other non-process chemicals, in varying compositions. Wet chemical methods involving the lime cycle have been used for recycling pulping chemicals for decades with only slight changes in the process. Aqueous electrochemical methods have been researched in the past, but require an ion selective membrane, prone to fouling and requiring high cell voltages due to the low conductivity of black liquor (1). A recovery process of an electrochemical

molten salt nature has not been investigated until now (1). The molten sodium carbonate electrochemistry has been adapted from research on the Molten Carbonate Fuel Cell (MCFC). Bartlett and Johnson (2) have investigated the carbonate reduction (cathode) and oxidation (anode) in a lithium-sodium carbonate eutectic on an inert anode. Dunks (3) has also investigated the electrochemical reactions in sodium carbonate melts on carbon anodes. Both report various mechanisms and intermediates that conclude to the production of sodium oxide.

The electrochemical path to a sodium hydroxide solution involves the preferential reduction of sodium carbonate, in the molten state, to a sodium oxide, also in the molten state [1-3]. Product gases would include carbon monoxide and carbon dioxide, and extent of carbonate conversion could be monitored by their flowrates. Addition of water to the sodium oxide after the electrochemical process would yield a sodium hydroxide solution [4]. The extension from the MCFC research has been the addition of sodium sulfide to the melt with the anticipation that a sulfur balance would be maintained in the smelt.



$$E^\circ_{1200\text{K}} = -1.57 \text{ Volts}$$



[1,7,8]. In comparison to the sodium carbonate oxidation/reduction on an inert anode [1,9,10], sulfur formation is favored by 0.66 Volts. Carbon anodes were used in the reported experiments to avoid producing elemental sulfur. Electrode technology transfer can be facilitated since carbon anodes are used on the industrial scale in the electrochemical production of aluminum from a molten salt bath.

## **Experimental**

### ***Materials***

Sodium carbonate (*anhydrous*, granular, 99.5% assay, VWR) was dried for 24 hours in an oven at 115°C prior to use. Sodium sulfide (anhydrous, 99.3% assay) was packaged under argon by Alfa Aesar and kept in a desiccator prior to use.

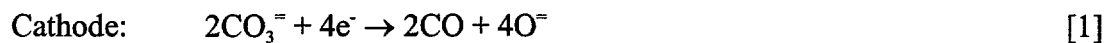
Industrial grade argon (Air Products) was used as the reactor purge gas, and a mixture of 5% CO, 15% CO<sub>2</sub>, and 80% nitrogen (Air Products) for analyzer calibration.

The molten salt mixture was contained in a flat-bottomed cylindrical alumina crucible (Coors 99.8 % Al<sub>2</sub>O<sub>3</sub>, 8.3 cm dia., 16 cm tall). Arched plates of similar alumina ceramic, 3 to 6 cm in height, 6 cm in length, served as an effective diffusion barrier with the purpose of hindering direct shuttling of electrochemical species between the two electrodes. A larger diameter (Coors, 99.8% Al<sub>2</sub>O<sub>3</sub>, 10.5 cm dia., 19.4 cm tall) crucible was used to contain the smelt in case of crucible fracture.

### ***Apparatus***

Figure 3 represents an overall view of the experimental apparatus. The electrochemical cell was contained within a steel reactor that sealed with bolts in a flange

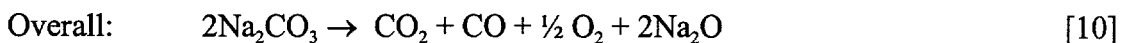
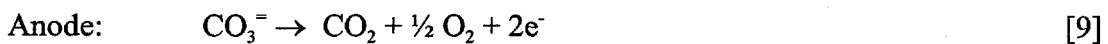
Comparison of equilibrium voltages ( $E^{\circ}_{1173K}$ ) based on Gibbs free energy of formation data (4) at 1200 K (926.85 °C) indicate that the carbonate reduction/oxidation [1-3] will be the preferred reaction with respect to sulfide reduction to carbon disulfide [1,5&6] on a carbon anode. Reaction 6 would not be favored since it requires a greater negative voltage with respect to the carbonate oxidation/reduction [1-3]. Calculations show that sulfide can electrochemically react to elemental sulfur (b.p. 444.6 °C) on an inert anode



$$E^{\circ}_{1200K} = -1.89 \text{ Volts}$$



$$E^{\circ}_{1200K} = -1.93 \text{ Volts}$$



$$E^{\circ}_{1200K} = -2.59 \text{ Volts}$$

and gasket assembly. A top loading electric crucible furnace (Lindbergh/Blue M) was raised around the fixed reactor system by use of a lab jack. *On the top of the reactor*, multiple ports equipped with plastic compression fittings (Swagelok) facilitated height adjustment of electrodes, purge port and thermocouple. The plastic fittings also provided electrical isolation of the electrodes from the reactor vessel. The purge gas was regulated with a mechanical bead flowmeter and the flowrate was determined using a bubble flowmeter. The exhaust gas was passed through a filtered condensate volume in order to capture smelt solid particulate ("fume"), then to a carbon monoxide and carbon dioxide analyzer (Infrared, Inc.). The condensate bottle also served to capture the excess waters of hydration that were not removed during the chemical pretreatment. The detectors were calibrated with inert argon gas to zero, and a carbon monoxide (5%), carbon dioxide (15%) mixture for the span.

Figure 4 shows the molten salt electrochemical cell. The smelt and containment crucibles rested on *an Inconel plate, used for spacing*, on the bottom of the steel reactor. A two-electrode system with a separator was used. The cathode was a stainless steel solid rod (316, 1/4" diameter for sodium carbonate electrolysis, 440C, 1/2" diameter for synthetic smelt electrolysis, 36" length) and the anode was a carbon rod (1/2" diameter, 36" length, Poco Graphite). The effective geometric surface area of the electrodes could be individually adjusted by changing their heights and securing at the top of the reactor with the compression fittings. The upper lengths of the electrodes were exposed to the ambient conditions, which facilitated electrical connections via copper clamps. Electrical current was provided by a 25 Ampere DC power supply (TET Electronics, Model

AGROS 40-25) and digital multimeters (Protek, Model B-845) were connected in order to monitor the cell current and potential (voltage).

### ***Procedure***

Synthetic smelts were prepared as either all sodium carbonate (~300 grams) or with a composition of 80 mole %  $\text{Na}_2\text{CO}_3$  and 20 mole %  $\text{Na}_2\text{S}$  for a total loading of ~300 grams ( $\cong$  3 cm of smelt depth). The synthetic smelt was transferred into the alumina crucible with the ceramic separators in place. The electrodes were inserted into the top of the reactor and raised above the smelt. The salt loaded alumina cell was positioned in the bottom of the reactor, raised into place and bolted closed. The ceramic purge port (Omega Engineering,  $\frac{1}{4}$ " dia.) was secured 20-30 cm above the granular salts while the K-Type thermocouple sheathed in a closed bottom tube well (Omega Engineering,  $\frac{1}{4}$ " dia.) was positioned 1 cm from the bottom of the smelt crucible. The system was purged with argon (0.5 – 1.2 L/min) for 12 hours before the heating was initiated. The smelt was ramped to a temperature of 900 °C ( $\pm$  10 °C). After the smelt reached the desired temperature, the electrodes were adjusted to a depth of 2 - 3 cm in the smelt, and a low constant current below one Ampere was supplied to the electrochemical cell. The current was then incrementally raised to a predetermined value. As the electrochemical oxidation consumed the carbon anode, the effective surface area would change, which was compensated for by periodic gravity feeding (lowering) of the anode. Gas product evolution was manually logged during the experiment as a function of time, along with the current, potential, furnace temperature and cell temperature. Experimental measurements were entered onto a spreadsheet that facilitated data integration.

After a predetermined number of coulombs were passed through the smelt, the current was turned off and the electrodes were raised above the smelt level. The temperature was ramped down below the melting point of the smelt, and then allowed to cool for an additional 10-12 hours, *still under argon purge*. The reactor was opened and the crucible removed after near ambient conditions were attained. Masses of the crucible containing smelt and electrodes were recorded. Powder samples were taken from the smelt by a power drill *with a 0.5-inch wood drill bit*. Particulate was collected from the walls of the steel reactor and filter condensate bottle. The remaining solid smelt sample was dissolved with a known mass of deionized water. The solution was slowly dissolved with a propeller bar mounted to a vertical variable motor.

Wet analysis of the dissolved solution was performed by volumetric and potentiometric titration methods ( $\pm 5$  mole %) with standardized hydrochloric acid, similar to the ABC titration used in the pulp and paper industry. Powder samples from the post-experimental smelt were heat tested to detect for the presence of sulfur (m.p. 120 °C).

Theoretical calculations were performed from gas analysis data to determine the expected amount of sodium oxide product predicted by equations 1 and 2, and subsequent moles of sodium hydroxide in solution [4]. Since the carbonate ion has been assumed the only source of oxygen in the melt, any oxygen containing molecules detected in the exit gas were assumed the products of the oxidation and reduction of carbonate. The stoichiometric ratio between the carbon monoxide and carbon dioxide may not obey the electrochemically predicted ratio due to non-equilibrium conditions, and the carbon rich

system. Therefore it was necessary to identify the amount of "Oxygen" leaving the system, and base the oxide formation prediction on the identified amount of oxygen in the product gas. The electrochemical oxidation/reduction reactions [1-3] predict that 4 Faradays of electrons will electrochemically convert 4 moles of  $\text{Na}_2\text{CO}_3$  into 3 moles  $\text{CO}_2$  and 2 moles of CO product gas and 4 moles  $\text{Na}_2\text{O}$  in the melt to balance. When the 4 moles of sodium oxide are dissolved into water, they create 8 moles of sodium hydroxide [4], creating an overall molar increase, yet maintaining a balance of sodium. This relationship predicts one mole of sodium hydroxide produced for one mole of "Oxygen" detected as product gas. If reaction of the sodium oxide product proceeds, it would produce additional oxygen gas products. The predicted value for sodium hydroxide will be higher than analytic result due to this increased gas detection.

The total volume of the product gases was approximated from combined experimental data and inlet purge rate. The densities of gases at standard conditions ( $0^\circ\text{C}$ , 1 atm) (5) were scaled to the ambient room temperature of the analyzers by the Ideal Gas Law to convert product gas volumes into product masses and subsequent moles of sodium hydroxide ( $\pm 5$  mole %, based on electrochemical gas production duration).

$$\text{Moles NaOH} = \sum_i ((v_i) (\text{gas volume}_i) (\text{gas density}_i) (\text{Molecular Weight}_i)^{-1}) \quad [11]$$

$$v_i = 1 \text{ for CO, } = 2 \text{ for CO}_2$$

## Results and discussion

The initial conditions for three experiments are listed in Table 1. Titration analyses of the final smelt are reported in Table 2. Experiment A demonstrates the small thermal effects (gas production) of the sodium carbonate melt (Figure 5) and titrations

could not detect measurable amounts of sodium hydroxide. Experiment B, the sodium carbonate electrolysis (Figures 6 & 7) produced 20.28 grams (0.507 mole) of sodium hydroxide (Table 2) and generated a magnitude more product gas (Table 3) with respect to Experiment A. The electrolysis of a synthetic smelt (Figures 8 & 9) was proved feasible in Experiment C by producing 25.88 grams (0.647 mole) of sodium hydroxide and 17.18 grams (0.156 mole) of sodium polysulfide. Sodium carbonate fume formation was observed along with mass changes of the electrodes (Table 4). Theoretical compositions of the smelt based on gas analysis data (Table 5) predicted *slightly* higher sodium hydroxide than found by titrations indicating the *slight* consumption of the sodium oxide product. Current densities and efficiencies are reported (Table 6) for the sodium carbonate oxidation and reduction reactions [1-3].

***Experiment A: Sodium Carbonate Melt, No Electricity***

A "blank" experiment was necessary in order to determine the volume of non-electrochemical (oxygen containing) product gas in the form of carbon monoxide and carbon dioxide. The electrochemical cell was loaded with 2.81 moles of sodium carbonate (Table 1) and was heated to 900°C where it was maintained for 120 minutes (Figure 5). The inlet purge rate was 1.2 L/min. and located 20 cm above the smelt bed. Two possible sources of background gas production have been identified as the product of the thermal decomposition of sodium carbonate [12] and the formation of a self-passivating aluminate (m.p. 1800°C) layer from the reaction between sodium carbonate and the alumina cell components [13], (6).





The characteristic peak in carbon dioxide during the heat up operation was observed in Experiments A & C with a maximum in the range of 300 – 500 °C and accounted for 75 mole % of the gases produced during Experiment A (Table 3). The heat-up peaks have been assumed to be attributed to reaction 13.

It is not likely that the thermal decomposition played a significant role since the titrations could not detect measurable amounts of sodium hydroxide (Table 2). The potentiometric titration did in fact show the low presence of the hydrogen carbonate ion (bicarbonate, 0.14 mole %) which can be expected in an aqueous carbonate solution.

#### ***Experiment B: Molten Sodium Carbonate Electrolysis***

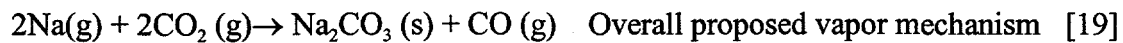
The electrochemical cell was assembled with a sodium carbonate loading of 2.782 moles and 252 cm<sup>2</sup> of separator surface area (Table 1). The cell was placed in the reactor, under an argon purge rate of 0.538 L/min. at a location 25 cm above smelt surface. Product gases were observed to decrease to steady background levels. The current was initiated when the temperature approached 900°C (m.p. Na<sub>2</sub>CO<sub>3</sub>, 851°C). There was an immediate increased response in carbon monoxide and carbon dioxide production when electrolysis began (Figures 6 & 7), indicating the occurrence of the desired electrochemical sodium carbonate reactions [1 & 2]. The CO<sub>2</sub> level dropped after twenty minutes when the current was increased from 10 to 15 Amperes, and a white fume was observed four minutes later.

Two possibilities have been identified to explain this phenomena. Electrical heating of the smelt was observed upon electrolysis, and it can be assumed that the electrodes are much hotter than the bulk of the molten salt. Carbon dioxide produced at the carbon anode surface may chemically react with carbon anode, consuming an additional carbon to produce carbon monoxide [14]. This reaction would be one explanation for the occurrence of non-stoichiometric gas proportions as well as excess mass loss of the anode (Table 4).



The second possibility for the drop of carbon dioxide would result from the fume formation phenomena observed in the recovery boiler. Fume formation collected from the inside of the reactor and filter bottle was determined to be less than 2 mole % (Table 4) and analytic titration analysis verified that it was sodium carbonate. The exact mechanism for fume formation may involve radical chemistry and/or a simple temperature dependent equilibrium, and likely has its origins in the thermal decomposition of sodium carbonate. The sodium oxide ( $\text{Na}_2\text{O}$ , sublimes  $1275^\circ\text{C}$ ) product of the thermal decomposition [12] or electrochemical production [1] may chemically react with free carbon in system to form elemental sodium (b.p.  $882^\circ\text{C}$ ) and carbon monoxide [15], (3). Interesting vapor chemistry, a subject beyond the purpose of this paper, between elemental sodium, carbon monoxide, carbon dioxide, and an array of





high temperature compounds may be the pathway to sodium carbonate fume formation [16 - 18]. Equation 19 represents the overall mechanism proposed for the formation of sodium carbonate fume and gives an explanation of the non-stoichiometric amounts of CO/CO<sub>2</sub> as predicted by the electrochemistry. Experimental evidence has shown the presence of elemental sodium as observed by small orange sparks that occurred in the presence of fume when hot product (exit) gases from the top of the reactor were sprayed into the ambient air. The sparking phenomenon was not observed in the filter bottle or at the exit of the gas detectors, even though fume was evident at both locations, despite collection by the filter paper, alluding to the fumes small size. This observation supports the idea that if elemental sodium was being produced, then it was recombining by an unknown mechanism to reform sodium carbonate in the vapor phase and result in a fine molecular fume. *The sodium carbonate fume did not coat the walls of the reactor until a point higher than the purge ports initial location. The fume formation has been observed to be temperature dependent since the fume did not begin to coat the inside of the reactor until approximately 30 cm above the smelt surface. The temperature profile quickly decreases towards the top of the reactor due to the top loading nature of the furnace, and the corresponding initial fume formation temperature has been estimated to be in the range of 400 – 600 °C. The highly erratic frequency of the exit flow rate was observed*

*and can be rationalized by volume change upon phase transition between solid melt to vapor products back to solid fume.*

As the current was ceased, the gas products immediately decreased. Enough current to obtain near 100% current efficiency (2.75 Faradays for 2.78 moles of  $\text{Na}_2\text{CO}_3$ , reactions 1-3) was passed through the cell. The electrodes and thermocouple were immediately raised above the smelt to avoid being frozen into it during the cool down.

Theoretical calculations (Table 5) from the gas analysis and results obtained by the titrations (Table 2) are in good comparison, indicating that the chemical oxide consumption may not be a significant reaction. A slight decrease in sodium content (due to fuming) of the melt is observed (Table 1 & 2), although it is within experimental error.

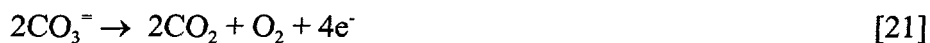
### ***Experiment C: Electrolysis of a Synthetic Molten Smelt***

Process feasibility required the electrolysis of sodium carbonate in the presence of sodium sulfide. The electrochemical cell was loaded with an 80 mole %  $\text{Na}_2\text{CO}_3$ , 20 mole %  $\text{Na}_2\text{S}$  mixture that forms a eutectic melt with a melting temperature of  $\sim 750^\circ\text{C}$ . Cell separator area was decreased to  $108\text{ cm}^2$  since systematic problems of port and electrode insertion were encountered in the sodium carbonate electrolysis with high separator area. Argon purge rate was set at 1.046 L/min. and placed within 20 cm of the smelt surface. The carbon dioxide peak characteristic of the aluminate passivation was observed during the cell heat-up (Figure 8). Hydrogen sulfide was briefly detected during heat up which can be explained by sodium sulfide reaction with water from either waters of hydration not removed by chemical pretreatment or by the salts absorption of ambient moisture during preparation of the cell. The sulfur loss was observed as a slight smelt

sulfur decrease (Tables 1 & 2) within the error of the experiment. The H<sub>2</sub>S was short lived and ceased 1.5 hours before electrolysis was started. The amount of hydrogen sulfide produced could not be quantified. No other sulfur gases were detected during the experiment by the olfactory sense. Electrolysis was initiated at 772°C, and after a short lag time, gas production began to increase, with more CO<sub>2</sub> generated than CO (Figures 8 & 9). The temperature of the melt increased 100°C during the first 40 minutes of electrolysis, during which the product gas levels continued to also increase. After this point, both CO and CO<sub>2</sub> levels began to decrease while a constant current of 18 Amperes was maintained. Fume formation was again observed four minutes after the current was raised from 18 to 20 Amperes. The decrease in CO<sub>2</sub> (875 °C) production appears to coincide with the boiling point of sodium (b.p. 882 °C). The electrodes were occasionally adjusted to facilitate gravity feeding of the carbon anode into the melt and to check the molten state of the smelt. At the 333 minute point on Figures 8 & 9, the purge port was lowered within 8 cm of the smelt surface to assist in removal of product gas from the cell. When the gas levels dropped to near background levels, the current was decreased to one Ampere and then increased to 10 Amperes. The gas evolution was observed to increase and follow a trend of near equal volumes of CO and CO<sub>2</sub> (favoring the CO<sub>2</sub>), which could have been caused by the reorientation of the purge stream towards the smelt surface. The change in CO/CO<sub>2</sub> ratios with change in the purge location and strongly indicates that purge location (and flowrate) can have a strong effect on the process chemistry. The peaking behavior of the product gases at constant current was observed multiple times and was coupled with a slight increase in the measured potential. This can be attributed to electrode passivation by products or decrease in local reactant

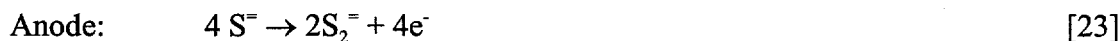
concentration. At the point 626 minutes on Figures 8 & 9, the polarities of the electrodes were momentarily switched to observe the effects on gas production. After the polarity switch, the gas production increased for 150 minutes then plateaued for 20 minutes before decreasing under constant current. The current was terminated during the decrease of gas production and the electrodes were removed from the melt.

25.88 grams (0.647 moles) of sodium hydroxide were produced (Table 2). Theoretical calculations based on gas analysis predicted more sodium hydroxide than was found in the melt by titration methods (Tables 5 & 2). Since the gas analysis calculation was based on two moles of oxygen as gas products per one mole as oxide in the melt from one mole of carbonate electrolyzed, there would be additional hydroxide predicted if the oxide product was converted to gaseous products. In addition to the chemical reaction of sodium oxide and carbon [15], Lorenz and Janz (7) describe an electrochemical reaction on an inert anode that favors the oxide consuming oxidation [20] over the carbonate oxidation [21] at low current densities. The equivalent oxide consumption reaction on a carbon anode as represented in equation 22. To deter the oxide products from further electrochemical reactions, a cell compartment separator was utilized in these experiments. The oxide produced at the cathode can be consumed if



allowed to reach the anode. The separator's purpose was to prevent product shuttling by dividing the cell into compartments in order to keep the oxide products away from the anode. The carbonate only electrolysis had approximately twice the amount of separator material than in the synthetic smelt experiment. The decreased separation efficiency can explain the discrepancy between predicted and actual hydroxide (Tables 2 & 5), although the difference is within the experimental margin. Consumption of the oxide can be considered a current inefficiency that can be lowered with improved separator and cell design and proper operating window.

Potentiometric titrations displayed an additional endpoint at a pH of 8.0 to the routine ABC titration, which has been reported to be indicative of solutions containing polysulfides (8). Thermodynamic consideration of the electrochemical polysulfide formation and carbonate reduction [1,23 & 24] versus carbonate reduction & oxidation [1-3] demonstrates an equilibrium voltage difference of 160 mV, favoring the latter.



$$E_{1200\text{K}}^0 = -1.73 \text{ Volts}$$

Production of polysulfides would lead to current inefficiencies and could explain the "peaking" behavior of gas evolution observed due to electrode passivation. Powder samples from the solid smelt and fume were heat tested between 100 – 150 °C and no melting of the solid was observed, indicating that elemental sulfur was not present.

Overall current efficiencies based on the desired sodium carbonate electrochemical reactions (1-3) are reported in Table 6. The low efficiencies can be attributed to the combined effects of additional electrochemical reactions and dissolution of the stainless steel cathode into the molten smelt, as observed in both electrolytic experiments (Table 4). Stainless steel metals (Fe, Ni, Cr, Mo) in the melt could dramatically increase the electronic conductivity in the melt and therefore suppress electrochemical reactions. The sodium carbonate reformation reactions that may be occurring in the vapor phase to form fume [13] can also occur in the melt (shuttling). These sodium carbonate reformation mechanisms attribute to the current inefficiencies depending on the melts equilibrium condition and solubility of carbon dioxide in the melt.

The desired sodium carbonate electrochemical reactions have been shown to occur at low current efficiencies and sodium hydroxide product has been confirmed by titration analysis. Cell design modification including separation scheme, purge flowrate/location and electrode materials should all lead to improving current efficiency. More detailed knowledge of the molten salt reaction mechanisms are currently being investigated by electroanalytical methods. Analysis of this nature will allow development of a potential window that will favor the carbonate reactions, thereby reducing current inefficiencies by oxide consumption and polysulfide formation.

### **Comparison of the electrolytic process with the conventional process**

Figure 10 shows a summary of a direct comparison between the conventional causticizing process and the proposed electrolytical causticizing process. The energy

savings are very significant (the system boundary for calculating these savings is the mill). The operating cost savings are strongly dependent on the price of fuel oil vs. electricity purchased by the mill. While currently no significant operating cost savings are predicted, this may change drastically if fossil fuel prices increase, or if more electricity is generated within the mill using new combustion technologies such as combined-cycle black liquor gasification.

## **Conclusions**

The fundamental feasibility of a new process for causticizing of kraft smelt has been shown.

The occurrence of oxygen containing gas generation upon applied electrical current (Figures 5 – 9) demonstrates the feasibility that, in the molten state, sodium carbonate can be electrolytically converted to sodium oxide (and subsequently to sodium hydroxide) while in the presence of sodium sulfide. Initial conditions and results are reported in Tables 1-6. The smelt shows to maintain a balance on sulfur within experimental error attributed to hydrogen sulfide generation during heat up and a slight sodium loss due to sodium carbonate fume. The current efficiencies include electronic conduction from dissolved electrode materials, further reaction of sodium oxide product due to shuttling, and polysulfide formation. Vapor chemistry, including phenomena of fume formation, can be effected by the electrochemical operation. The cell design of this batch process can be modified to reduce these current inefficiencies and fume formation by improving separator design, electrode selection, purge location and flowrate.

Operating cost estimates are close to the costs of the existing traditional process, but will change in favor of the electrolytic process if fossil fuel prices rise, or if co-generation of electricity in the mill increases. Very significant energy savings in regard to energy used in the mill are estimated.

## Table of Figures

Figure 1: Conventional chemical recovery.....	24
Figure 2: Conventional furnace with electrolytical causticizing .....	25
Figure 3: Molten salt electrolysis experimental apparatus.....	26
Figure 4: Electrochemical molten salt cell.....	27
Figure 5: Experiment A, <b>no</b> electrolysis, molten sodium carbonate product gas and temperature data. (Blank for thermal effects). The temperature is normalized by 200°C.....	28
Figure 6: Experiment B, electrolysis of molten Na <sub>2</sub> CO <sub>3</sub> , product gas data. ....	29
Figure 7: Experiment B, electrolysis of molten Na <sub>2</sub> CO <sub>3</sub> , smelt temperature and current/potential data. The temperature is normalized by 100 °C.....	30
Figure 9: Experiment C, electrolysis of synthetic smelt (molten Na <sub>2</sub> CO <sub>3</sub> & Na <sub>2</sub> S), smelt temperature and current/potential data. The temperature is normalized by 100°C. ...	32
Figure 10: Side-by side comparison of energy demand and operating cost for the electrolytical causticizing process vs. the conventional causticizing process.....	33

## Table of Tables

Table 1: Initial conditions.....	34
Table 2: Final smelt composition form titration analysis. ....	35
Table 3: Final results of gas production.....	36
Table 4: Mass/mole amount of collected fume and electrode changes.....	37
Table 5: Theoretical composition of final smelt based on gas analysis data and assumed electrochemistry.....	38
Table 6: Electrical results.....	39

Figures

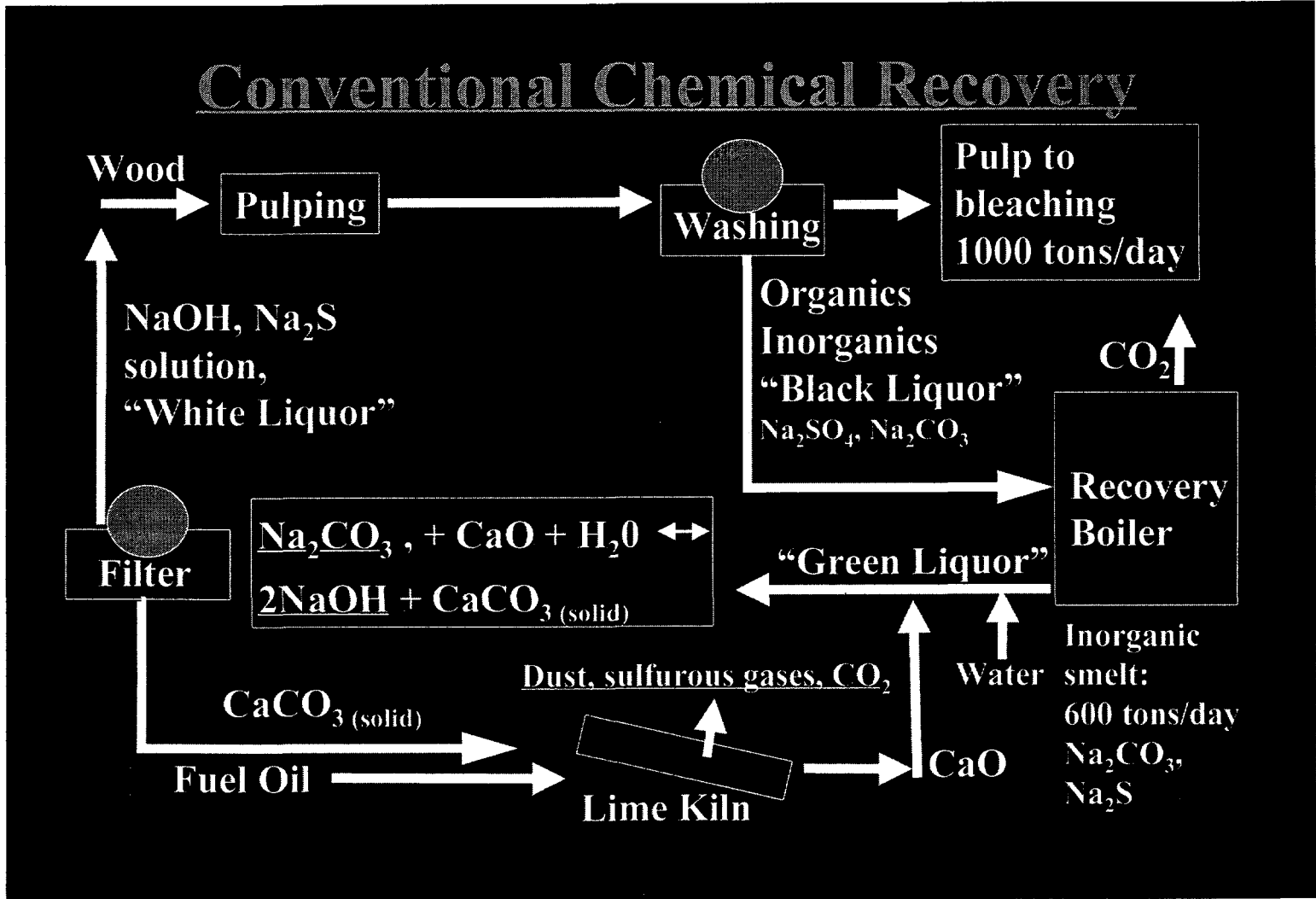


Figure 1: Conventional chemical recovery.

# Conv. Furnace + Electrolytical Causticizing

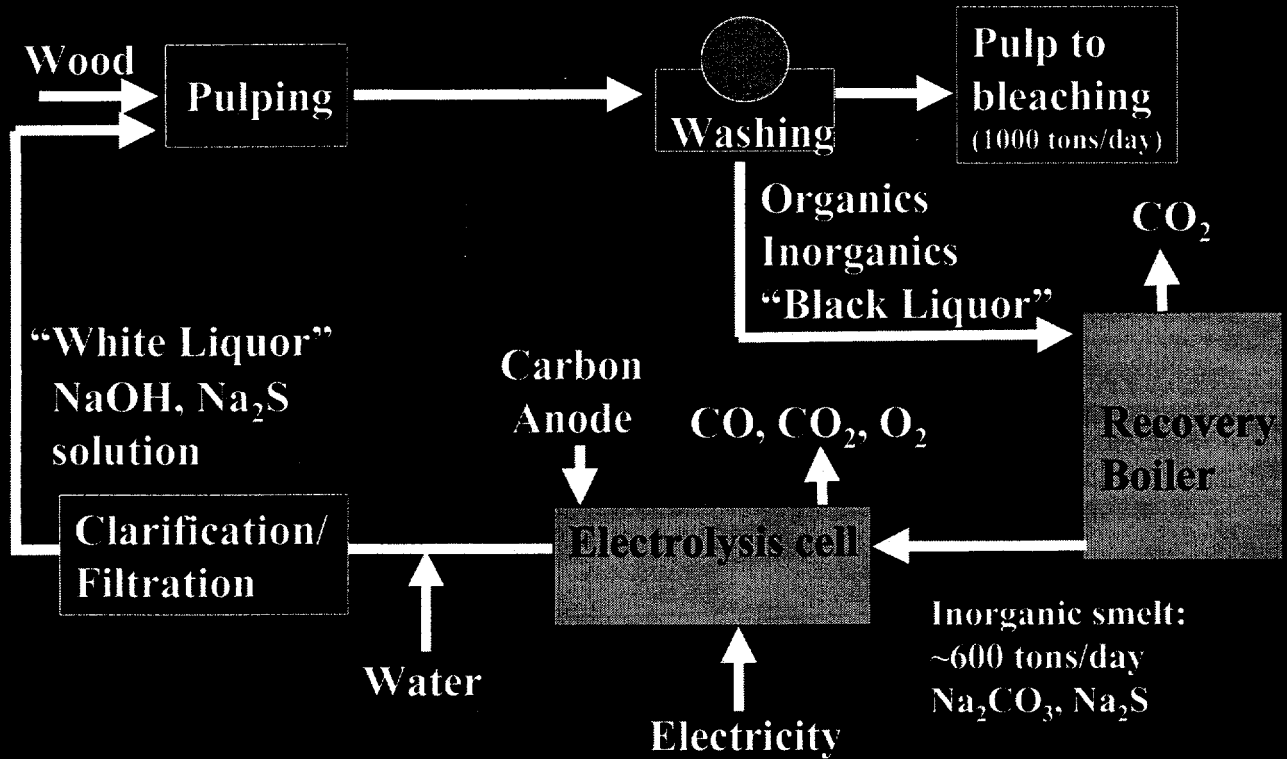


Figure 2: Conventional furnace with electrolytical causticizing

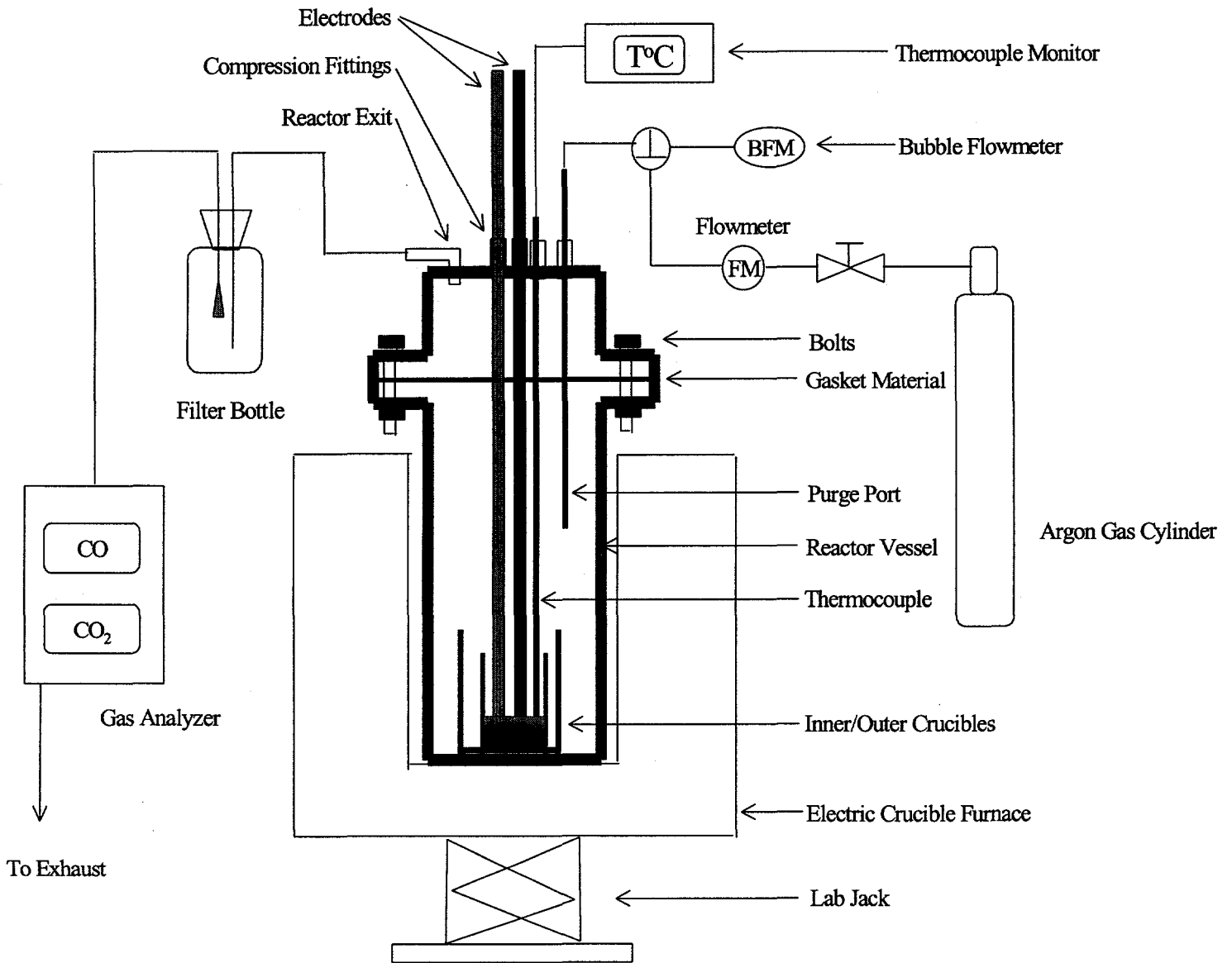


Figure 3: Molten salt electrolysis experimental apparatus.

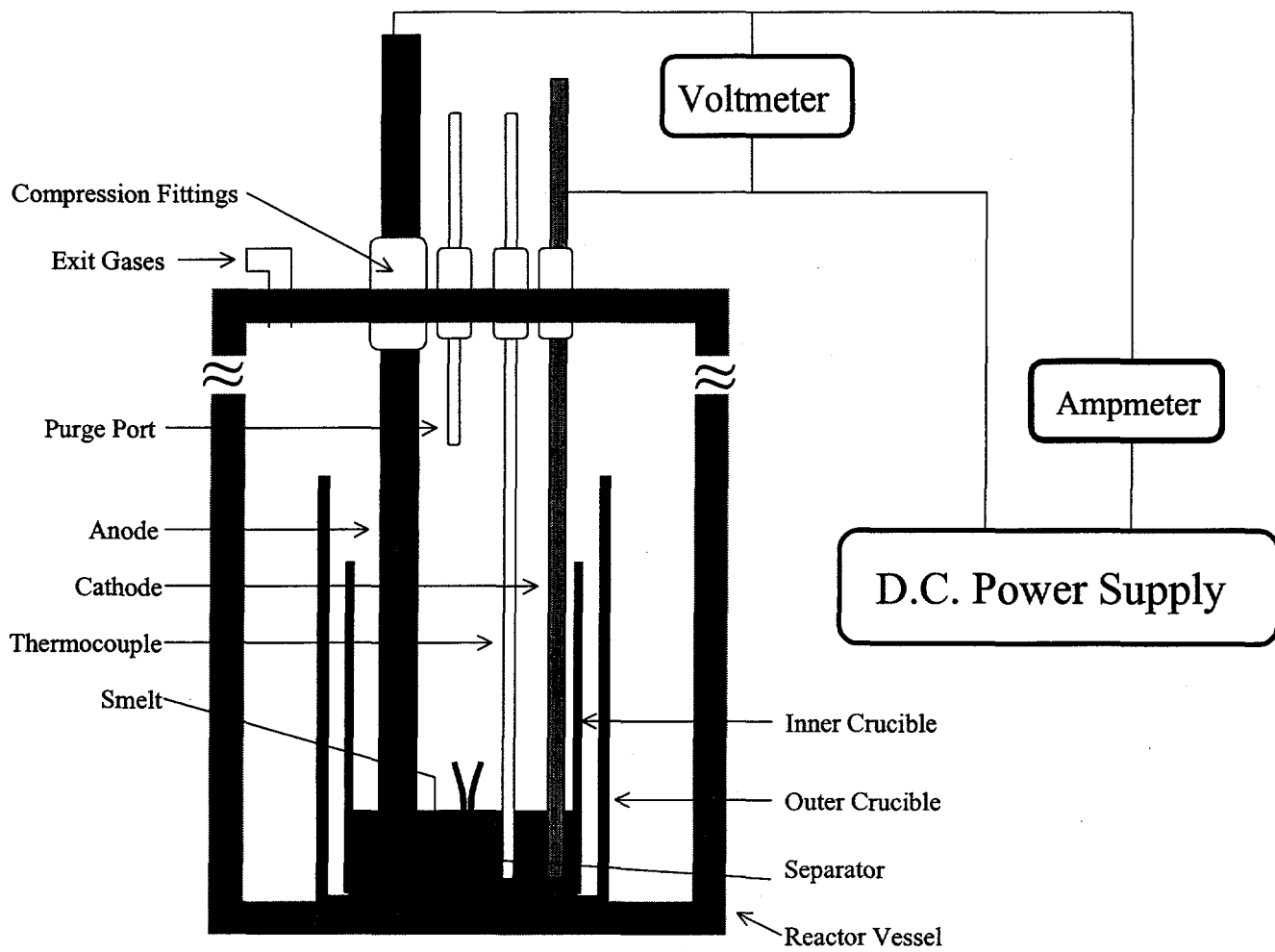


Figure 4: Electrochemical molten salt cell.

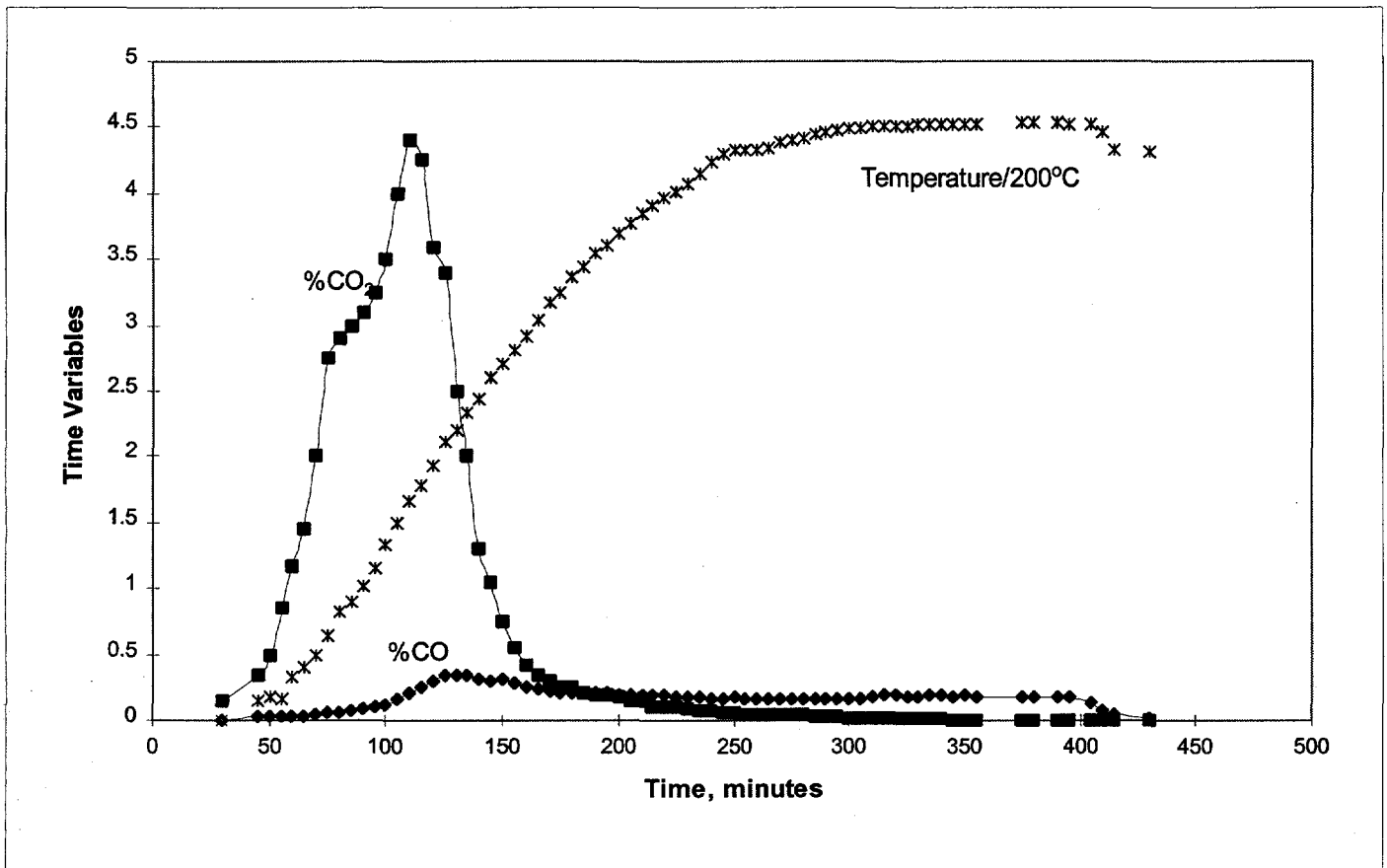


Figure 5: Experiment A, no electrolysis, molten sodium carbonate product gas and temperature data. (Blank for thermal effects). The temperature is normalized by 200°C.

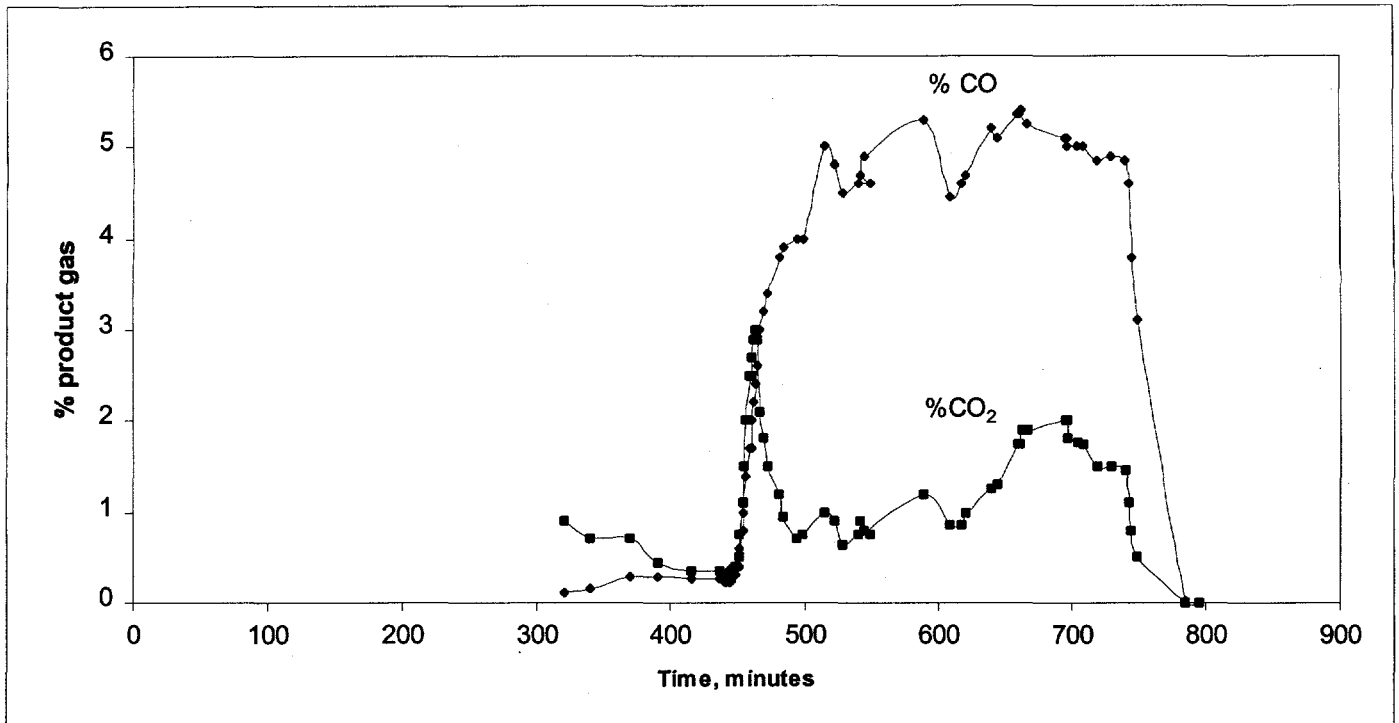


Figure 6: Experiment B, electrolysis of molten Na<sub>2</sub>CO<sub>3</sub>, product gas data.

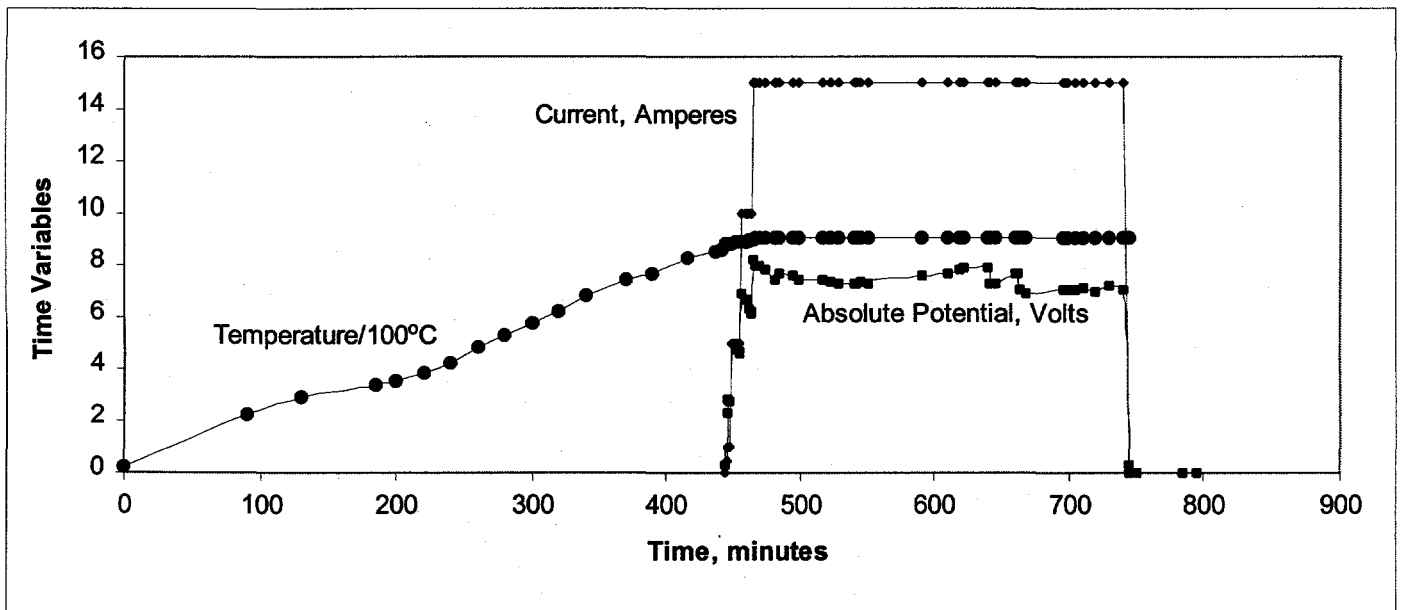


Figure 7: Experiment B, electrolysis of molten  $\text{Na}_2\text{CO}_3$ , smelt temperature and current/potential data. The temperature is normalized by  $100^\circ\text{C}$

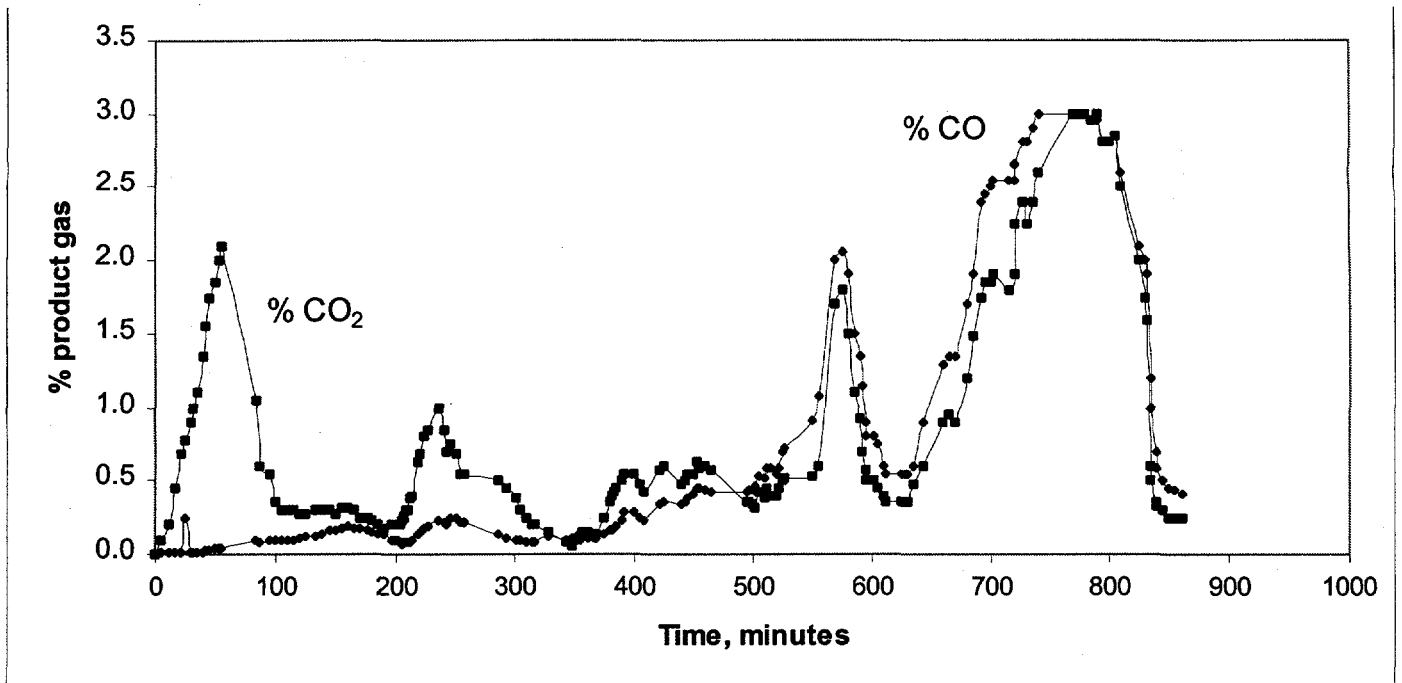


Figure 8: Experiment C, electrolysis of synthetic smelt (molten Na<sub>2</sub>CO<sub>3</sub> & Na<sub>2</sub>S).

Product gas data.

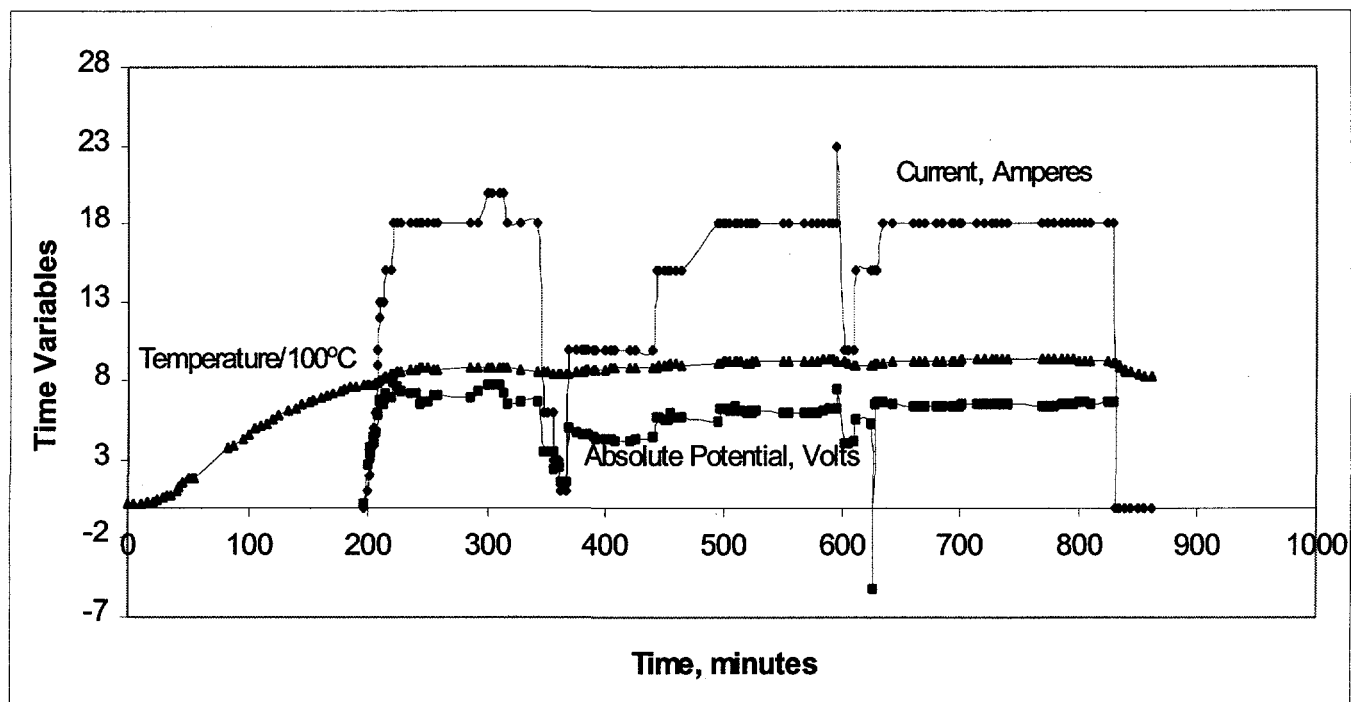


Figure 9: Experiment C, electrolysis of synthetic smelt (molten  $\text{Na}_2\text{CO}_3$  &  $\text{Na}_2\text{S}$ ), smelt temperature and current/potential data. The temperature is normalized by  $100^\circ\text{C}$ .

<b>ESTIMATED OPERATING COSTS AND ENERGY DEMAND</b>			
<b>Conventional vs. electrochemical causticizing</b>			
J. Winnick, P. Pfromm, Proposal: "Electrolytic Causticizing of Kraft Smelt"			
DOE Agenda 2020, Capital Effectiveness			
<b>Base: 1000 tons of pulp produced per day</b>			
<b>General assumptions:</b>			
Electrical energy:	0.035	\$/kWh	
Fuel oil, kiln:	2.5	\$/million BTU	
Smelt:	570	tons/day	
Sodium carbonate:	67	wt% of smelt	
Causticizing efficiency needed:	85	%	
Active CaO needed	241	kg/ton of pulp	
	<b>Operating Cost</b>		<b>Energy Demand</b>
<b>Conventional causticizing</b>			
Fuel oil, kiln:	7.00E+06	Btu/ton CaO	352 kWh/ton of pulp
Fuel oil cost:	4.2175	\$/ton of pulp	
Electrical power (pumping etc.)	1.5	megawatt	0.04 kWh/ton of pulp
Electrical energy cost:	1.26	\$/ton of pulp	
Makeup lime:	13	tons/day	
Makeup lime cost:	1.95	\$/ton of pulp	
Steam:	0.5	\$/ton of pulp	neglected
Maintenance	1.9	\$/ton of pulp	
Labor	1.5	\$/ton of pulp	
<b>TOTAL, CONVENTIONAL:</b>	<b>11.3</b>	<b>\$/ton of pulp</b>	<b>352 kWh/ton of pulp</b>
<b>Electrochemical causticizing:</b>			
Electrical energy from amount of carbonate to causticize:			
1 volt cell voltage,	6840790.422	Amps needed per day	
Electrical power (80% current efficiency):	205.22	kWh/ton of pulp	205.2 kWh, electrolytical
<b>Electrochemical Electrical energy cost:</b>	<b>7.18</b>	<b>\$/ton of pulp</b>	
Drive Electrical costs	0.32	\$/ton of pulp	assume 1/4 of conventional
Maintenance	0.95	\$/ton of pulp	assume 1/2 of conventional
Labor	0.75	\$/ton of pulp	assume 1/4 of conventional
Carbon anodes	cost currently not available, but material is a waste from petroleum processing		
<b>TOTAL, ELECTROLYTIC:</b>	<b>9.2</b>	<b>\$/ton of pulp</b>	<b>205 kWh/ton of pulp</b>
<b>Savings using new process:</b>	<b>19 %</b>	<b>operating cost savings</b>	<b>42 % energy savings</b>
(conventional =100%)			
Kraft production in the US per year	50000000	tons per year	
Energy saved per ton	147	kWh	
1 btu=	2.93E-04	kwh	
Energy saved per ton	5.02E+05	btu	
Energy saved in the US per year	2.51E+13	btu	
<b>Energy saved in the US per year</b>	<b>2.51E+04</b>	<b>billion BTU per year</b>	
if traditional causticizing is replaced by electrolytical causticizing.			
<b>Conclusion</b>			
<b>Operating cost comparison depends strongly on costs for electricity vs. oil</b>			
<b>No credit taken for:</b>			
<b>possibility to increase causticizing to high levels and convert sulfate to sulfide</b>			
<b>(increased production through decreased deadload)</b>			
<b>Environmental and process advantages, and energy savings warrant research.</b>			
(energy savings are offset in regard to op. cost by increased energy costs for electricity vs. fuel oil)			

Figure 10: Side-by side comparison of energy demand and operating cost for the electrolytical causticizing process vs. the conventional causticizing process.

## Tables

		Table 1: Initial Conditions									
		Na <sub>2</sub> CO <sub>3</sub>	NaOH	Na <sub>2</sub> S			Anode	Cathode	Separator	Purge	
							Diameter Inch	Diameter Inch	Surface Area cm <sup>2</sup>	Rate L/min, Ar	
Na <sub>2</sub> CO <sub>3</sub> No Electrolysis	moles	2.806	0.000		5.613	Na				1.200	
	mole %	100.000	0.000								
Na <sub>2</sub> CO <sub>3</sub> Electrolysis	moles	2.782	0.000		5.564	Na	0.50	0.25	252	0.528	
	mole %	100.000	0.000								
Na <sub>2</sub> CO <sub>3</sub> & Na <sub>2</sub> S Electrolysis	moles	2.112	0.000	0.978	6.180	Na	0.50	0.50	108	1.046	
	mole %	69.643	0.000	30.357							S
											Na/S

Table 1: Initial conditions.

		Table 2: Final, Titration Analysis					
		Na <sub>2</sub> CO <sub>3</sub>	NaOH	Na <sub>2</sub> S	Na <sub>2</sub> S <sub>2</sub>		
Na <sub>2</sub> CO <sub>3</sub> No Electrolysis	mole (+/- 0.1 mole) mole %	2.802 99.862	0.000 0.000			5.605	Na
Na <sub>2</sub> CO <sub>3</sub> Electrolysis	mole (+/- 0.1 mole) mole %	2.503 83.154	0.507 16.846			5.512	Na
Na <sub>2</sub> CO <sub>3</sub> & Na <sub>2</sub> S Electrolysis	mole (+/- 0.1 mole) mole %	1.794 55.375	0.647 19.979	0.642 19.835	0.156 4.811	5.831 0.954 6.111	Na S Na/S

Table 2: Final smelt composition from titration analysis.

		Table 3: Final, Gas Products			
		Carbon Monoxide, CO		Carbon Dioxide, CO <sub>2</sub>	
		Full Run	Electrolytic Run	Full Run	Electrolytic Run
Na <sub>2</sub> CO <sub>3</sub> No Electrolysis	mole (+/- 0.1 mole) grams	0.033		0.011	0.138
		0.937		0.481 (w/o CO <sub>2</sub> Peak)	6.080 (CO <sub>2</sub> Peak)
Na <sub>2</sub> CO <sub>3</sub> Electrolysis	mole (+/- 0.1 mole) grams	0.344	0.331	0.141	0.093
		9.630	9.266	6.223	4.091
Na <sub>2</sub> CO <sub>3</sub> & Na <sub>2</sub> S Electrolysis	mole (+/- 0.1 mole) grams	0.312	0.295	0.296	0.280
		8.751	8.267	13.039	12.315

Table 3: Final results of gas production.

		Table 4		
		Dust	Changes	
			Cathode	Anode
Na <sub>2</sub> CO <sub>3</sub> No Electrolysis	grams mole (+/- 0.1 mole)	0.000 0.000		
Na <sub>2</sub> CO <sub>3</sub> Electrolysis	grams mole (+/- 0.1 mole)	4.250 0.040	3.910	8.960 0.746
Na <sub>2</sub> CO <sub>3</sub> & Na <sub>2</sub> S Electrolysis	grams mole (+/- 0.1 mole)	4.720 0.045	22.680	3.300 0.275

Table 4: Mass/mole amount of collected fume and electrode changes.

Table 6			
	Current Density Ampere/cm <sup>2</sup>	Faradays Passed	% Electrical Efficiency
Na <sub>2</sub> CO <sub>3</sub> No Electrolysis			
Na <sub>2</sub> CO <sub>3</sub> Electrolysis	2.38	2.747	9.228
Na <sub>2</sub> CO <sub>3</sub> & Na <sub>2</sub> S Electrolysis	1.36	6.650	4.865

Table 6: Electrical results.

---

## Literature Cited

1. OLOMAN, C., "Electrochemical Processing for the Pulp & Paper Industry", 1<sup>st</sup> ed., The Electrochemical Consultancy, England (1996).
2. BARTLETT, H.E. and JOHNSON, K.E., "Electrochemical Studies in Molten  $\text{Li}_2\text{CO}_3\text{-Na}_2\text{CO}_3$ ", *J. Electrochem. Soc.* 14(5):456-461(1967).
3. DUNKS, G.B., "Electrochemical Studies of Molten Sodium Carbonate in Relation to Graphite Oxidation", 1983 International Conference on Coal Science, 457-460 (1983).
4. LIDE, D.R.Jr. (Editor), "Journal of Physical and Chemical Reference Data, JANAF Thermochemical Tables", Third Edition, American Institute of Physics, Inc., New York (1986)."
5. GREEN, D.W. (Editor), "Perry's Chemical Engineering Handbook", Sixth Edition, McGraw-Hill (1984).
6. DUNKS, G.B., STELMAN, D., and YOSIM, S.J., "Graphite Oxidation in Molten Sodium Carbonate", *Carbon* 18:365-370 (1980).
7. LORENZ, P.K. and JANZ, G.J., "Electrolysis of Molten Carbonates: Anodic and Cathodic Gas-Evolving Reactions", *Electrochem. Acta* 15:1025-1035 (1970).
8. DORRIS, G.M., and ULOTH, V.C., "Analysis of Oxidized White Liquors. Part II: Potentiometric Titrations for the Determination of Polysulphides and Sulphoxy Anions" *J. Pulp Paper Sci.* 20(9):J242-248 (1994)